6-16-2007

Detection, attribution, and sensitivity of trends toward earlier streamflow in the Sierra Nevada

Edwin P. Maurer
Santa Clara University, emaurer@scu.edu

Iris T. Stewart-Frey

Celine Bonfils

Philip B. Duffy

Daniel R. Cayan

Recommended Citation

Maurer, E.P., I.T. Stewart, C. Bonfils, P.B. Duffy, and D. Cayan, 2007, Detection, attribution, and sensitivity of trends toward earlier streamflow in the Sierra Nevada, J. Geophysical Research 112, D11118, doi:10.1029/2006JD008088.

Detection, attribution, and sensitivity of trends toward earlier streamflow in the Sierra Nevada

E. P. Maurer,[1] I. T. Stewart,[2] C. Bonfils,[3] P. B. Duffy,[3,4] and D. Cayan[5,6]

Received 29 September 2006; revised 16 March 2007; accepted 30 March 2007; published 13 June 2007.

[1] Observed changes in the timing of snowmelt dominated streamflow in the western United States are often linked to anthropogenic or other external causes. We assess whether observed streamflow timing changes can be statistically attributed to external forcing, or whether they still lie within the bounds of natural (internal) variability for four large Sierra Nevada (CA) basins, at inflow points to major reservoirs. Streamflow timing is measured by "center timing" (CT), the day when half the annual flow has passed a given point. We use a physically based hydrology model driven by meteorological input from a global climate model to quantify the natural variability in CT trends. Estimated 50-year trends in CT due to natural climate variability often exceed estimated actual CT trends from 1950 to 1999. Thus, although observed trends in CT to date may be statistically significant, they cannot yet be statistically attributed to external influences on climate. We estimate that projected CT changes at the four major reservoir inflows will, with 90% confidence, exceed those from natural variability within 1–4 decades or 4–8 decades, depending on rates of future greenhouse gas emissions. To identify areas most likely to exhibit CT changes in response to rising temperatures, we calculate changes in CT under temperature increases from 1 to 5°. We find that areas with average winter temperatures between −2°C and −4°C are most likely to respond with significant CT shifts. Correspondingly, elevations from 2000 to 2800 m are most sensitive to temperature increases, with CT changes exceeding 45 days (earlier) relative to 1961–1990.

Citation: Maurer, E. P., I. T. Stewart, C. Bonfils, P. B. Duffy, and D. Cayan (2007), Detection, attribution, and sensitivity of trends toward earlier streamflow in the Sierra Nevada, *J. Geophys. Res.*, *112*, D11118, doi:10.1029/2006JD008088.

1. Introduction

[2] California, like many regions that rely on snow for water supply, is particularly vulnerable to a warming climate. With rain and snow occurring in winter and water use peaking in summer, water managers face the annual challenge of storing the winter precipitation for use later in the year. The single largest storage of water in the state is the snowpack, which on 1 April (typically used as the date indicative of the peak in snow accumulation) contains on average about 13 km^3 of water for the areas draining into the Sacramento, San Joaquin river system [*Cayan et al.*, 2007], which can be compared to the volume of Lake Shasta, the largest man-made reservoir in California of 5.5 km^3.

[3] Some of the earliest investigations into impacts of global warming on California highlighted the temperature-driven impacts on snow as robust and important, including a greater proportion of precipitation falling as rain instead of snow and earlier melt of snow [*Gleick*, 1987; *Lettenmaier and Gan*, 1990]. Both effects have been detected in the observational record in the western United States and have been attributed to recent rising temperatures much more than to changes in precipitation [*Knowles et al.*, 2006]. The compound effect of this warming is for streamflow to occur earlier in the year. Recent studies have documented this phenomenon in observational records in different snow-dependent regions [*Hodgkins et al.*, 2003; *López-Moreno and García-Ruiz*, 2004; *Mote et al.*, 2005; *Regonda et al.*, 2005] and attributed this largely to increasing temperatures (as opposed to changes in precipitation) in the western United States over the past half century [*Stewart et al.*, 2005, hereinafter referred to as S05].

[4] An earlier arrival of streamflow has profound implications for water management in California, which has inspired many recent studies of global warming and water resources in California [*Brekke et al.*, 2004; *Hayhoe et al.*, 2004; *Maurer and Duffy*, 2005; *Stewart et al.*, 2004; *Tanaka et al.*, 2006]. In general, water managers account for the

[1]Civil Engineering Department, Santa Clara University, Santa Clara, California, USA.
[2]Environmental Studies Program, Santa Clara University, Santa Clara, California, USA.
[3]School of Natural Sciences, University of California, Merced, California, USA.
[4]Also at Lawrence Livermore National Laboratory, Livermore, California, USA.
[5]Climate Research Division, Scripps Institution of Oceanography, University of California, San Diego, La Jolla, California, USA.
[6]Also at Water Resources Division, U.S. Geological Survey, La Jolla, California, USA.

0148-0227/07/2006JD008088

water stored as snow as a natural reservoir and anticipate the arrival of the snowmelt in the late spring and early summer. They can thus leave vacated space in reservoirs to capture winter storm runoff, providing flood control benefits. As the winter storm season ends the snow begins to melt, providing runoff that can fill the reservoirs for summer water supply for irrigation and urban use and environmental releases. A shift in streamflow timing disrupts this system, increasing the conflict between providing both water supply and flood control. Recent evidence suggests that under future warming the system would not be capable of reliably meeting current demands [*Van Rheenen et al.*, 2004; *Vicuna et al.*, 2007].

[5] Orographic effects in the Sierra Nevada [*Dettinger et al.*, 2004] and temperature lapse rates produce an elevational dependence to projected and observed CT shifts. The shifts to earlier streamflow timing projected by *Maurer* [2007], using an ensemble of model and emissions scenario projections, show the shift for the higher-elevation basins accelerating toward the end of the 21st century as temperature increases. *Knowles and Cayan* [2004] illustrated, for one future climate projection, that the impact of warming on snow in California is likely to be most evident at elevations between 1300 and 2700 m. This is because lower elevations are already rain-dominated and elevations above 2700 m may remain below freezing even with warming temperatures. *Knowles et al.* [2006] demonstrate that observed changes toward more precipitation falling as rain as opposed to snow in the western United States have occurred at lower and moderate elevations with relatively thin snowpacks. Thus it is not surprising that *Howat and Tulaczyk* [2005] computed a lower sensitivity of snow to warming using a statistical model based on historic snow observations with greatest concentration between 2600 and 3200 m.

[6] In a study specifically aimed at quantifying historic CT shifts, S05 showed that while observed tendencies toward earlier streamflow timing (for snow-dominated streams) are consistent across the western United States, the magnitude of the shift over the past five decades is greater at lower-elevation basins compared to those above roughly 2000 m. However, because the domain of S05 was large enough to where latitudinal and other climate variations were also important, the impacts of elevation alone on streamflow timing could not be separated.

[7] Natural variability will produce some trends in CT over the relatively short record of historical observations. It is possible to determine statistically whether individual station CT trends over the past decades are significantly different from zero, as shown by S05. However, without a much longer historical record, it is not possible to establish either the interannual variability of the previous decades or the variability of trends in streamflow timing. This means that we do not have the observational records necessary to determine whether any observed trends result from natural variability, or whether they may be due to anthropogenic or other external forcing.

[8] The main focus of this study is the Sacramento–San Joaquin Basin that drains the western Sierra Nevada (CA) and in particular inflow points to major reservoirs, where water managers will ultimately need to adapt to streamflow timing changes. These inflow points represent a key part of California's water supply system, and have larger drainage basins, ranging in area from 4,000 to 10,000 km^2, that include portions that may not be snow-dominated. In contrast, S05 included primarily smaller, snow-dominated basins, and within California included a total of 24 basins with an average drainage area of approximately 600 km^2. Our focus on larger river basins, which include both rain- and snow-dominated portions, will be expected to show a lower sensitivity of CT shifts to temperature increases than exclusively snow-dominated basins.

[9] Building on these previous studies, the goal of this work is to address the following two questions: (1) Since natural variability will produce varying 50-year trends in streamflow timing even in a stable climate, at what magnitude would an observed trend exceed natural variability with high confidence, and thus be attributable to some external influence (such as increased greenhouse gases)? (2) Where can the most significant changes in streamflow timing be expected under a 1°–5°C warming (as is projected for California for the next century)? This second question is aimed at providing insight into identifying drainage basins most vulnerable to timing changes in a warming climate.

2. Methods

2.1. Study Region

[10] The focus for our study is California's Sacramento–San Joaquin basin, the heart of the multibillion dollar agricultural industry of California and home to the fastest growing metropolitan areas in the state. The water that drains from the western slopes of the Sierra Nevada supplies the extensive system of dams and reservoirs serving the water demands of much of the state. Figure 1 shows four stream locations, all inflows to large reservoirs, which are the focus of this study. These are the same points used by *Maurer* [2007]. The southern two basins contain more high-elevation areas than the northern two, such that a broad range of basin elevations is represented.

2.2. Hydrologic Model

[11] For simulating the land surface response to climate in this study, the hydrologic model employed is the variable infiltration capacity (VIC) model [*Liang et al.*, 1994, 1996]. VIC is a macroscale, distributed, physically based hydrologic model that balances both surface energy and water budgets over a grid mesh, typically at resolutions ranging from a fraction of a degree to several degrees latitude by longitude. The VIC model allows the use of a "mosaic" scheme, representing elevation zones within each grid cell, allowing subgrid-scale topographical detail to be statistically represented. This is an important feature when simulating the accumulation and ablation of snow in more complex terrain such as in California.

[12] The VIC model has been successfully applied in many settings, from global to river basin scale [*Abdulla et al.*, 1996; *Maurer et al.*, 2001, 2002; *Nijssen et al.*, 1997], as well as in several studies of hydrologic impacts of climate change [*Christensen et al.*, 2004; *Hayhoe et al.*, 2004; *Maurer and Duffy*, 2005; *Nijssen et al.*, 2001; *Payne et al.*, 2004; *Wood et al.*, 2004]. For this study, the model was run at a 1/8° reso- resolution (measuring about 140 km^2 per grid cell) over the Sacramento–San Joaquin basin. Sources of elevation, soil

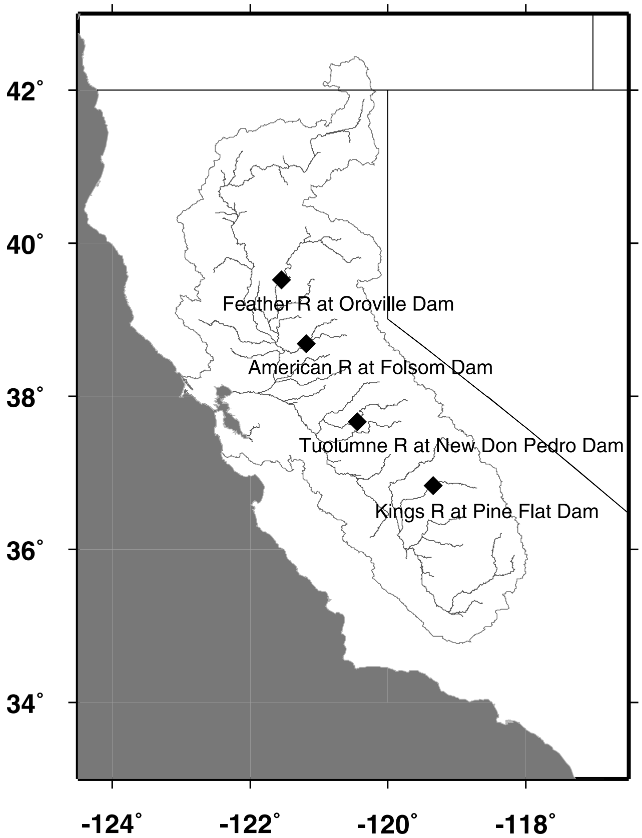

Figure 1. Sacramento–San Joaquin basin, showing four stream gauge locations at the outlets of key watersheds discussed in the text.

and vegetation coverage used in the VIC hydrology model are described in detail by *Maurer et al.* [2002].

[13] Unlike weather forecasting hydrology models, which are extensively calibrated at each streamflow simulation site [*Peck*, 1976; *Smith et al.*, 2003], the VIC model is typically only minimally calibrated, relying on its physically based parameterizations to plausibly simulate the hydrologic cycle. Figure 2 shows the model simulation at the four strategic points in Figure 1 for the period 1980 through 1989, driven by the gridded observed meteorology of *Maurer et al.* [2002], after a minimal manual calibration using the period 1990–1999. The overall bias is below 10% at all points, and the annual cycle of streamflow is accurately represented. *Hamlet et al.* [2005] and *Mote et al.* [2005] have identified biases in snow simulations using the VIC model in the Sierra Nevada, attributing the biases to several possible causes. These causes include biases in the meteorological data driving the model, and the discrepancies in comparing point snow measurements (often in open areas) with simulated snow averaged over a 1/8° grid cell (which includes areas with overstory). Meteorological data suffer from poor coverage in mountainous regions, and interpolation to a spatially continuous grid requires the assumption of a lapse rate which may not be appropriate for any particular day. Given the physically based representation of hydrologic processes in the VIC model, and the accuracy of simulated streamflow when driven by the observationally based meteorology, we argue that the representation of the water cycle components in the basins should be reasonable.

2.3. Global Climate Model Simulation and Downscaling

[14] The coupled global ocean-atmosphere-land general circulation model (or global climate model, GCM) output used in this study is from the Parallel Climate Model (PCM) [*Washington et al.*, 2000]. The PCM control run used here is run B06.62, which consists of a simulation approximately 1000 years in length, beginning at a year arbitrarily numbered 100. The output were then screened to avoid missing data (missing in the archived data files), resulting in complete simulation years 451 to 1079 forming the continuous 629-year control run for subsequent analysis in this study. This preindustrial control run, which uses constant 1870 atmospheric composition to force the model, had been performed in support of Intergovernmental Panel on Climate Change assessments (IPCC AR4). We also use the monthly PCM temperature and precipitation output for the 20th century for 1950–1979, from the "20c3m" "run1" IPCC AR4 experiment. All monthly PCM output was linearly interpolated to a regular 2° grid prior to additional processing as described below.

[15] For illustration, Figure 3 compares the cumulative distribution functions (CDFs), at a single 2° grid cell, the monthly PCM temperature output for 1950–1979 along with the aggregated gridded observed data [*Maurer et al.*, 2002] for the same grid cell. This shows that, especially in the late winter through early summer the PCM at this single point underestimates natural interannual variability of surface air temperature. Similar analysis of other grid points (not shown) reveals overestimation of natural variability toward the southern end of the domain. This is in qualitative agreement with C. Bonfils et al. (Identification of external influences on temperatures in California, submitted to *Climate Change*, 2006, hereinafter referred to as Bonfils et al., submitted manuscript, 2006), who found that on average the simulated interannual variability corresponds well with observations over California as a whole. The 20th century PCM simulation includes the most important sources of variability, including greenhouse gases, sulfate aerosol direct effects, volcanic aerosols, tropospheric and stratospheric ozone, and solar irradiance [*Santer et al.*, 2006]. Thus we assume the underestimation or overestimation of variability at any grid point is a model tendency, and not due to a lack of time-varying external forcing of variability. In other words, we assume any bias in interannual variability exhibited by the PCM in this 20th century simulation would also occur in the PCM control simulation at the same grid point.

[16] The purpose of Figure 3 is not to demonstrate regional GCM biases, which have been well documented by others [e.g., *Covey et al.*, 2003; *Zhu et al.*, 2004], but primarily to illustrate how the differences between raw GCM output and observations are corrected in this study. Because of the bias in interannual variability (and other statistical moments) in the raw GCM output, we apply the bias correction technique originally developed by *Wood et al.* [2002] for using global model forecast output for long-range streamflow forecasting. The method was later adapted for use in studies examining the hydrologic impacts of climate change [*Christensen et al.*, 2004; *Hayhoe et al.*, 2004;

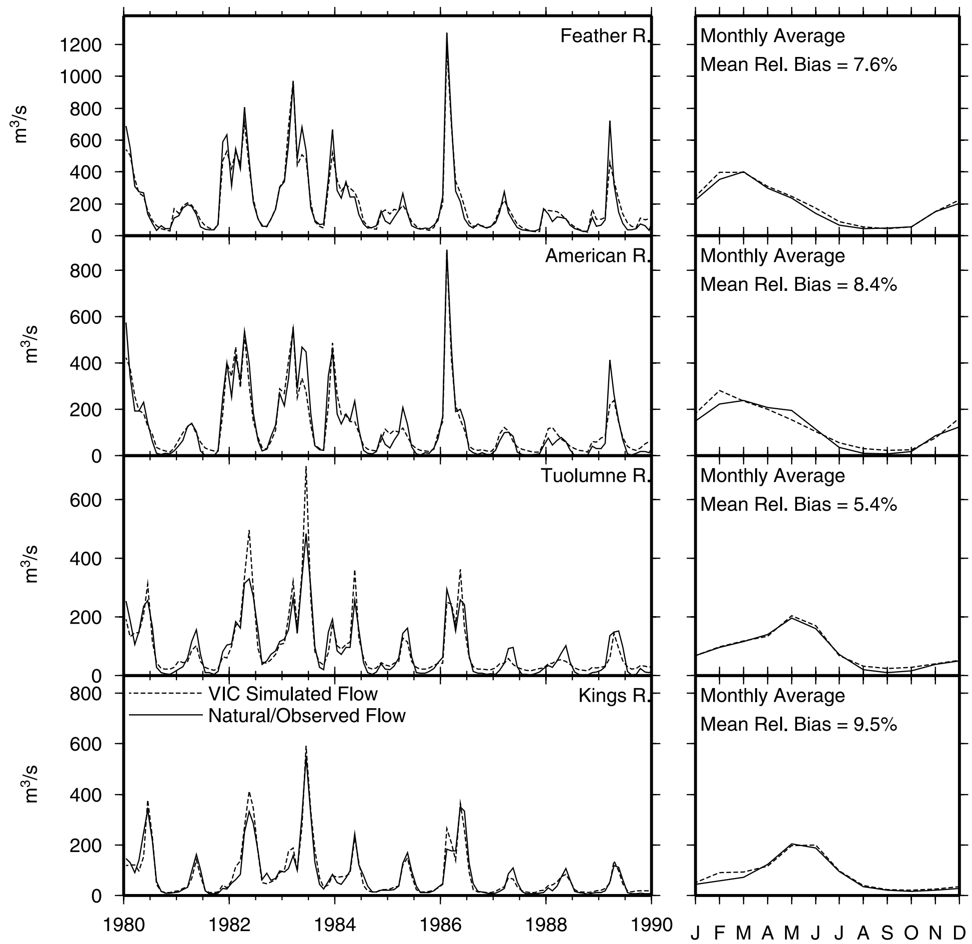

Figure 2. VIC model performance at the four key streamflow locations discussed in the text. (left) Monthly flow time series and (right) 10-year average of each month.

Maurer and Duffy, 2005; *Payne et al.*, 2004; *Van Rheenen et al.*, 2004; *Wood et al.*, 2004]. This is an empirical statistical technique that maps precipitation and temperature during a historical period (1950–1979 for this study) from the GCM to the concurrent historical record. For precipitation and temperature, empirical cumulative distribution functions are built for each of 12 months for each of the 2° grid cells for both the gridded observations and the GCM for the climatological period. For the entire simulation period the quantiles for GCM simulated variables are then mapped to the same quantiles for the observations. For example, if for one grid point the GCM temperature value in January of 1950 is equal to the median GCM value for January for 1950–1979, it is transformed to the median value for the gridded January observations for 1950–1979. For temperature, the linear trend is removed prior to this bias correction and replaced afterward, to avoid increasing sampling at the tails of the CDF as temperatures rise. The same bias correction is then applied to the entire control run. The resulting bias-corrected GCM output displays identical mean and variability (at each GCM grid point) as observations for the 1950–1979 period, but the statistical properties can change throughout the control run as simulated by the GCM.

[17] To downscale the bias-corrected GCM output to a scale useful for hydrologic analysis, we use the method applied by *Wood et al.* [2002], which for each month interpolates the bias corrected GCM anomalies, expressed as a ratio (for precipitation) and shift (for temperature) relative to the 1950–1979 period at each GCM grid cell to the centers of 1/8° hydrologic model grid cells over California. These factors are then applied to the 1/8° gridded observed precipitation and temperature data. *Wood et al.* [2004] show that this statistical bias-correction/downscaling method performs comparably to more sophisticated dynamical downscaling approaches. Though some differences do appear, especially at high elevations where snow albedo-atmosphere feedback is important, these are less important hydrologically as runoff contributions from larger more heterogeneous areas are integrated.

2.4. Flow and Runoff Center Timing

[18] Center timing (CT) of flow is used as the measure of streamflow timing in this study. This is defined, as in S05, as the day marking the point at which half of the total annual flow (mass or volume of water) has passed the point on the stream. To avoid negative values, all days are indexed to the water year, defined as the period starting 1 October of the previous year through 30 September of the current year. In addition to streamflow, we analyze spatially distributed runoff, the runoff produced at each grid cell before it enters the stream channel system. In this case CT is

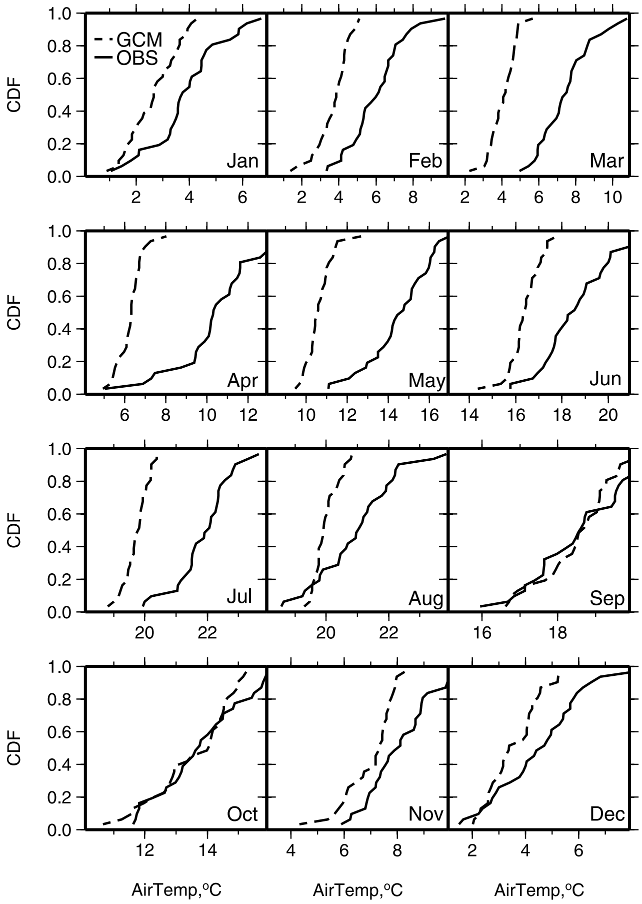

Figure 3. Cumulative distribution functions (CDFs) for monthly air temperature for 1950–1979 at one PCM model grid cell (centered at 39°N, 121°W). Ordinate values are probability of nonexceedance based on a Weibull plotting position. PCM simulations (dashed) and gridded observations (solid) are shown.

the date at which half of the annual runoff at any particular grid cell has been generated for each water year.

[19] We also use a method of determining whether a particular VIC model grid cell is rain or snow-dominated. We apply the same criterion as S05, which is based on a method of *Cayan et al.* [2001] for determining the onset of a spring snowmelt pulse. As implemented in S05 (and here), the mean flow for calendar days 9–248 is calculated and the minimum cumulative departure from this mean flow is then computed. The period covering calendar days 9 through 248 was chosen to broadly cover the snowmelt season over a range of warmer (lower elevation) to cooler (higher elevation) environments, from the middle of winter to the end of summer. This definition is thus able to capture fluctuations toward earlier as well as later snowmelt runoff timing. If the minimum departure falls between 15 February and 15 August for at least 30% of the years, the grid cell is determined to be snow-dominated.

3. Results and Discussion

[20] First, the PCM control simulation was analyzed to establish the natural (internal) variability of CT trends. This was then compared to observationally driven VIC-based CT trends during 1950–1999 at key locations. Following this, an investigation of CT sensitivity in the Sacramento–San Joaquin basin was performed.

3.1. Natural CT Trend Variability at Key Sites

[21] To estimate the natural variability of CT trends, the 629 year control simulation of the PCM (with model output processed as described above) was used to drive the VIC hydrology model, and the CT was computed for each year and for each streamflow site. We use the slope of a linear fit to characterize the trend in CT for each 50-year segment in the record (the start of successive 50-year segments are shifted 10 years, so the segments overlap, thus providing 58 complete segments).

[22] These sets of CT trends, in days per 50 years, are compiled into cumulative distribution functions, shown in Figure 4. As expected for the overall stationary temperatures prevalent during the control period, the mean CT trend is close to zero for all sites. The standard deviation is fairly consistent among the basins, varying from 12.4 to 15.1 days. Threshold exceedence values of Q10 are defined as the CT trends not exceeded 10% of the time. Alternatively stated, Q10 is the CT shift to earlier in the year that is only exceeded 10% of the time. Q10 varies from 17 to 19 days for the four stations considered, indicating that on the basis of this control run a 50-year trend in CT would need to shift 17–19 days earlier to achieve statistical confidence level of 90% (based on a one-sided test) that the trend exceeds natural variability.

[23] For reference this can be compared with S05 who found shifts in CT of 17.7 and 20.5 days earlier over the 1948 to 2002 period for two of their three sites (in the Sacramento–San Joaquin basin) achieving 90% confidence. It should be noted that the significance tests in S05 are qualitatively different from those above, representing only the confidence with which a linear trend for 1948–2002 is significantly different from zero, but not attributing the detected trend to either natural variability or external forcing

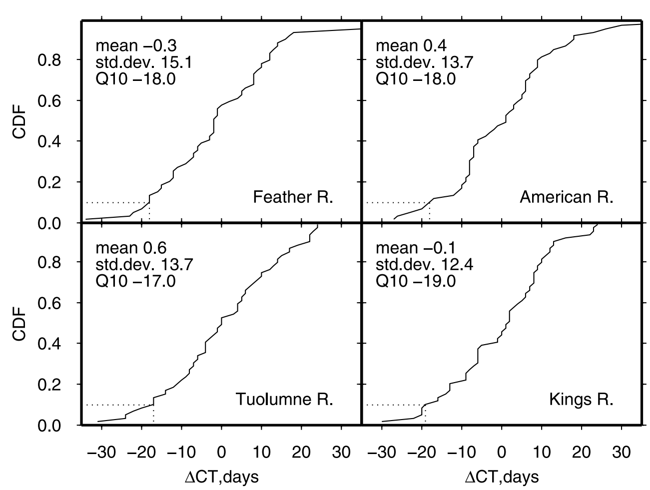

Figure 4. Cumulative distribution functions for CT trend (days/50 years) derived from temperature and precipitation from PCM control run. Q10 is the value not exceeded in 10% of the trend segments. Dotted lines indicate the Q10 value.

Table 1. Projected Changes in CT and Temperature From *Maurer* [2007][a]

Basin	Mid-High Emissions (A2)			Low Emissions (B1)		
	2011–2040	2041–2070	2071–2100	2011–2040	2041–2070	2071–2100
			ΔCT, days			
Feather R.	−14	**−18**	**−23**	−10	−11	**−17**
American R.	**−19**	**−23**	**−31**	−17	**−20**	**−26**
Tuolumne R.	−9	**−20**	**−33**	−10	**−14**	**−23**
Kings R.	−9	**−21**	**−36**	−8	**−16**	**−24**
			Temperature Change Relative to 1961–1990, °C			
All	1.0	2.2	3.7	1.0	1.7	2.3

[a]All changes are relative to a 1961–1990 base period. Values shown are ensemble means of projections by 11 GCMs. Bold values indicate positive attribution to external forcing.

(such as greenhouse gas-induced warming). It should also be noted that the streamflow points studied by S05 do not coincide with the four sites that are the focus of the current investigation. However, the relative consistency across the four diverse basins here suggests that these trends in S05 may approach the threshold for implying external forcing(s).

[24] The VIC hydrologic model driven by gridded observed climate data from 1950–1999 produces CT shifts at the four key sites of +4 days (later) to −9 days (earlier) for the period, all at confidence levels substantially below the upper limits probable from natural variability. Only the American River at Folsom (at ΔCT = −9 days) approaches an 80% confidence level, and this shift would need to double to achieve a 90% significance. This suggests that confident detection of (externally forced) streamflow timing shifts at these key locations, integrating runoff effects over relatively large and topographically varied river basins, is not possible on the basis of the short historical record. This raises the question of when (or at what temperature change) and where these shifts might be detectable with confidence. The remainder of this paper explores this question.

3.2. Projected CT Trends at Key Sites

[25] To begin addressing this question, Table 1 summarizes relevant results from *Maurer* [2007], who used an ensemble of 11 GCMs under two different future greenhouse gas emissions scenarios to drive a hydrologic model to project hydrologic changes, including CT shifts. All of the shifts in Table 1 demonstrated high confidence (>95%) as being different from zero. The shift between 2011–2040 and the 1961–1990 base period in Table 1 represents a 50-year trend, and thus can be compared to the Q10 thresholds developed in this study and shown in Figure 4. Comparing these, only the American River, under the A2 emission scenario, can produce a CT shift that is large enough for a positive detection of externally forced shift by early in the 21st century (bold values in Table 1 identify positive detection of external forcing). This indicates that in the near future CT in this basin is likely to be more vulnerable to temperature changes as compared to the other three basins in this study.

[26] CT shifts for mid- to late-21st century relative to 1961–1990 (Table 1), can be compared to those resulting from natural climate variability on longer (80- and 110-year) timescales. Table 2 summarizes the Q10 (90% confidence level) for natural variability from 50-, 80- and 110-year CT trends obtained using the PCM control simulation. As is expected for trends derived from longer samples from a stationary time series, the magnitudes of sampled (nonexternally forced) trends decrease with increasing timescale length, lowering the threshold of detectability. This is especially evident for the two basins containing more high-elevation area (Tuolumne and Kings Rivers), which tend to exhibit lower trend variability (discussed further below).

[27] As shown by Bonfils et al. (submitted manuscript, 2006), a detection of externally forced climate change can be negative on a 50-year timescale but positive on longer timescales because the amplitude of noise on longer timescales declines. Even in cases where smaller trends over shorter timescales are not attributable to external forcing, trends over longer timescales may be attributable to external forcing because, as timescale increases, the amplitude of noise can decline more rapidly than the magnitude of the signal (Bonfils et al., submitted manuscript, 2006). The enhanced detectability of external forcing at longer timescales, due to an improved signal-to-noise ratio, is evident in Table 2. One implication of this, not investigated here, is that CT shift over a longer observed record (1920–1999, for example) could be attributable to external forcing even where the 50-year trends included in this study are not.

[28] By mid-21st century, the mid-high emissions scenario produces shifts exceeding natural variability for all basins, with the higher-elevation Tuolumne and Kings River basins exhibiting CT shifts of twice that needed to attribute the trends to external influences, at 90% confidence. The shifts for the lower-elevation Feather River basin do not exhibit a CT trend confidently exceeding natural variability by mid-century under the lower emissions scenario. The other basins do, though by smaller margins than under mid-high emissions. All of the shifts by late-21st century achieve the

Table 2. Q10 (90% Confidence) Thresholds for CT Trends[a]

Basin	50-Year	80-Year	110-Year
Feather R.	−18	−16	−15
American R.	−18	−16	−15
Tuolumne R.	−17	−10	−8
Kings R.	−19	−11	−7

[a]Unit is days per N years. N is the length of time over which the trend is measured, to exceed natural variability.

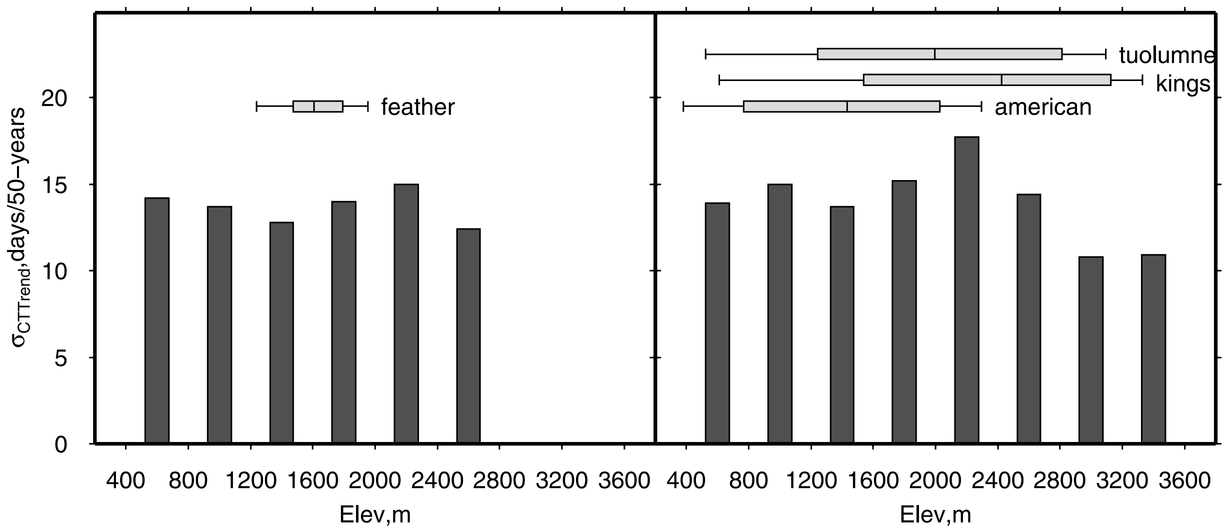

Figure 5. Standard deviation of the 50-year CT-trend for the PCM control run. (left) Areas north of latitude 39.5°N and (right) areas south of 39.5°N. Hypsometric data for the four key basins are shown, with the whiskers and bar representing 10, 25, 75 and 90 percentile elevations within each basin.

threshold for exceeding natural variability under both emissions scenarios.

[29] As shown above, the lower-elevation American River basin exhibits a greater tendency toward early detection of externally forced CT changes. For other locations the complexity of the topographic variability of the basins, and hence the varying hydrologic response to temperature, makes this detection more difficult. To evaluate this difference between basins, the standard deviations of the 50-year CT trends for the PCM control run were computed at each grid cell in the Sacramento–San Joaquin basin (Figure 5). This illustrates that the midelevation range of 2000–2400 m exhibits the greatest variability in 50-year trends. CT trends in this elevation range are influenced by combined effects of both temperature and precipitation variability, whereas at higher elevations temperature is less likely to influence CT (since warm anomalies may still lie below the freezing point) and at low elevations rainfall is dominant and temperature will not strongly affect CT. The lower variability of CT trends at high elevations also helps explain why detection thresholds are lower on longer timescales at higher elevations (Tuolumne and Kings Rivers), shown in Table 2. The implication is that although a basin might already be responding to climatic changes, the projected CT shift for these more vulnerable midelevations may also need to be larger to exceed the likely bounds of natural variability.

3.3. Vulnerability of CT to Temperature Changes at Different Elevations

[30] To investigate regions most likely to display significant temperature-driven CT changes, we apply different temperature shifts, applied uniformly at every 1/8° grid cell at every daily time step for all of 1961–1990. While precipitation amounts are unchanged from 1961 to 1990 in these simulations, its form will be different, with a greater proportion of rain compared to snow as temperature increases. The range of temperature increases used is compatible with the ranges projected for California in the 21st century of 1.3°–2.0°C by 2020–2049 and 2.3°–5.8°C by 2070–2099 [*Hayhoe et al.*, 2004].

[31] For any area where runoff is affected by snow, in the absence of precipitation changes, a shift in CT will be driven by temperature changes, especially in winter temperatures [*Bales et al.*, 2006], though other characteristics such as aspect [*Lundquist and Flint*, 2006] and forest canopy variability [*Bales et al.*, 2006] can also be significant factors. Figure 6 shows the CT shift for the grid cells in the study domain, where each cell is characterized by its mean (1961–1990) December–February temperature, and CT shifts are averaged over 2°C bins. As would be expected, the greatest sensitivity to temperature-induced CT shifts is for areas with winter temperatures below but near the freezing point. This was a motivation for *Bales et*

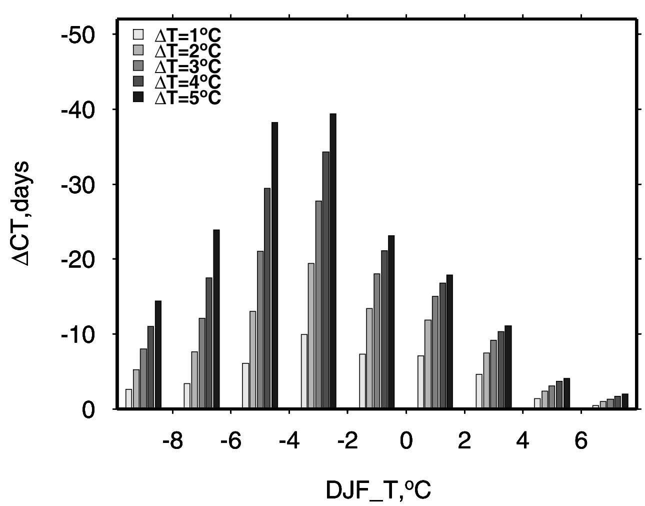

Figure 6. CT shift versus winter temperature, sorted into (1961–1990 mean) 2° bins. For each 2° bin of winter temperature, there is one bar for the shift in CT induced by the designated temperature increase over mean 1961–1990 values. Negative values indicate earlier.

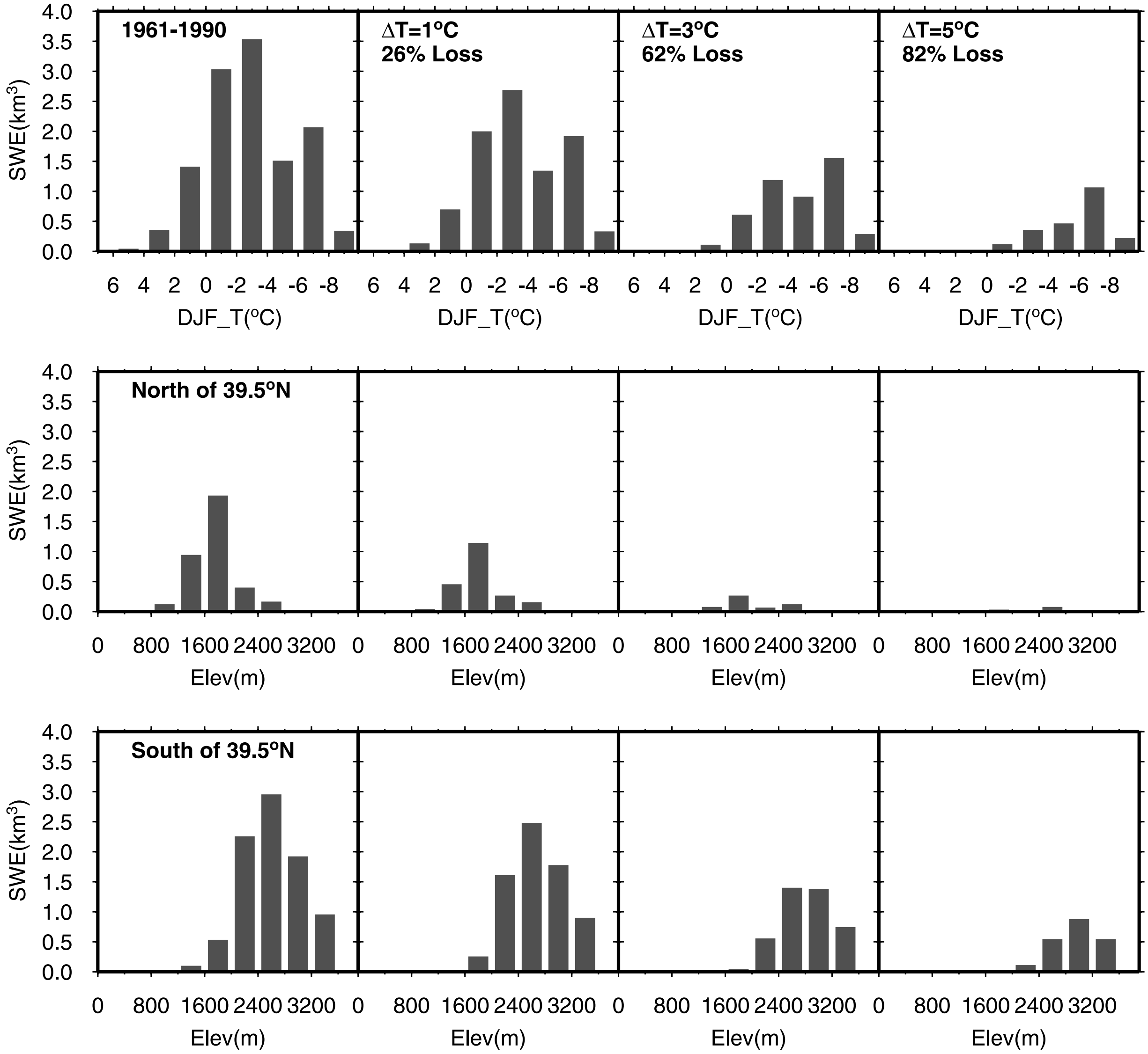

Figure 7. Volume of snow (as snow water equivalent, SWE) stored on 1 April by elevation for the base case of 1961–1990 and under different temperature increases. (top) SWE volume classified by winter (December–February, DJF) temperature. Domain classified by elevation (using 400 m bins) for areas (middle) north and (bottom) south of 39.5°N.

al. [2006] to map this region across the western United States. Figure 6 shows that for all of the designated increases in temperature, the greatest CT changes are projected for cells with 1961–1990 winter temperatures between −2°C and −4°C.

[32] Alternatively a more practical metric than temporally varying winter temperature may be a relatively static, physical basin characteristic such as elevation to characterize snow and snow-driven changes in the Sierra Nevada [*Howat and Tulaczyk*, 2005; *Knowles and Cayan*, 2004]. This is generally valid for climatological, as opposed to specific event, characterization [*Lundquist et al.*, 2004]. Complicating the use of elevation as a proxy for air temperature is that the domain of this study (Figure 1) covers a latitudinal range of 7.5°, large enough for there to be some influence of latitude on temperature. While for snow-driven effects elevation is substantially more important than latitude within the Sacramento–San Joaquin basin, as also found by *Howat and Tulaczyk* [2005], there is a latitudinal trend of winter (December–February) mean air temperature across the domain of approximately 4°C. To decrease this effect, the domain is split into a north (above latitude 39.5°N) and south (below 39.5°N) portion, similar to the approach of *Knowles and Cayan* [2004]. Within each of these portions of the domain, latitude explains less than 10% of the variance of winter temperature, while elevation explains 68% in the north and 95% in the south. In this way, elevation is assumed to be a valid surrogate for winter air temperature, allowing the classification of areas by a readily available physical property rather than a climatological characteristic.

[33] It is important to place the CT changes in Figure 6 in the context of the volume of water they represent. Figure 7 shows that the greatest storage, on 1 April, of snow for

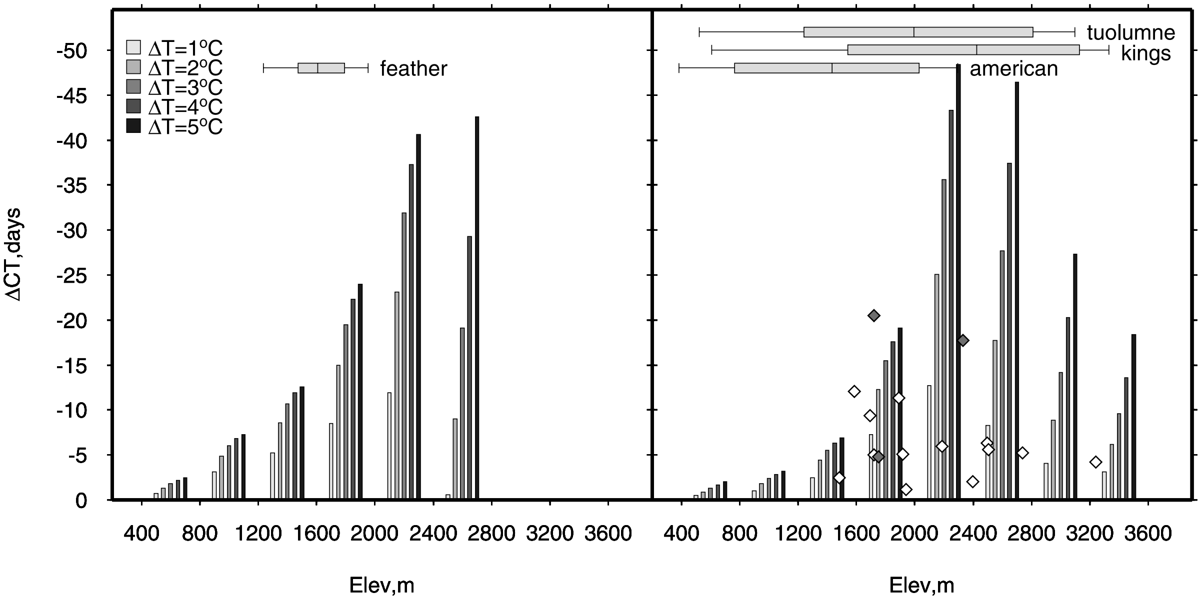

Figure 8. CT shift for individual VIC grid cells under specified temperature shifts relative to 1961–1990 for the (left) north and (right) south. *Stewart et al.* [2005] points (against basin average elevation) in the Sacramento–San Joaquin basin are added as diamonds, and darker solid diamonds indicate significance at the 90% level. Hypsometric data for the four key basins are as in Figure 5.

1961–1990 in the Sierra Nevada is in regions with winter temperatures between −2°C and −4°C, which coincides with the greatest CT changes (Figure 6) driven by increasing temperatures. While the 1961–1990 snow storage in regions with winter temperatures of 0°C to −2°C is nearly as great as for areas with winter temperatures from −2°C to −4°C, the CT shifts associated with loss of the snow are smaller, since there is a greater proportion of the 0°C to −2°C zone with a rain influence in 1961–1990. As illustrated by *Knowles and Cayan* [2004] and also shown in Figure 7, most of the historic (1961–1990) snow water is stored at elevations between 1600 and 2000 m north of 39.5°N, and between 2000 and 2800 m south of 39.5°N. Thus streamflow timing shifts at these elevations represent a greater water management issue, as the volume of water arriving earlier is much larger.

[34] To illustrate the response of different elevations to temperature change, Figure 8 shows the change in CT from 1961 to 1990 conditions for each of the VIC grid cells (averaged over 400 m elevation bins), for each fixed temperature shift. For comparison, the points corresponding to the basins in the study area used by S05 are included (which all fall south of 39.5°N). For reference, the average basin size of the S05 points here is 630 km^2, or approximately the size of four VIC grid cells. The basins for which S05 identified statistically significant CT shifts lie in the elevation range 1700–2300 m, which corresponds to the range of sensitivity at the lowest temperature increase in Figure 8. Figure 8 illustrates that as temperature rises the timing shift will both become more dramatic and affect higher-elevation areas. The greatest CT shifts, averaging 40–45 days earlier at a 5°C temperature increase (with some individual grid cells having shifts greater than 70 days), are at elevations between 2000 and 2400 m in both the north and south. It should be noted that this zone of the greatest shifts is the same as that of greatest natural variability in CT trends (Figure 5), indicating larger CT shifts will be needed to attribute the shifts to external causes. The coincidence of these is at least partially explained by the CT shift and the variability in CT trends both being influenced by proximity to the rain-snow threshold.

[35] The hypsometric data in Figure 8 illustrate that more than 90% of the Feather and American basins, and more than 50% of the Kings and Tuolumne basins lie below 2400 m elevation, and are thus highly sensitive to temperature increases of 1°–2°C above 1961–1990 levels. The hypsometric data also show that impacts in CT shift will be complicated at these sites, as they all include approximately 25–50% of their contributing area from lower-elevation, rain-dominated zones. The Tuolumne and Kings River basins, with median elevations above 2000 m, represent higher elevation and more snow-dominated basins. Similar to the findings presented here, *Maurer* [2007] also shows that by the end of the 21st century, CT shifts under two contrasting future emissions scenarios (Table 1) were significantly different at each of the higher-elevation basins, demonstrating greater temperature sensitivity at higher (2000–2800 m) elevations.

[36] The shift in CT can also be interpreted in light of whether contributing areas to a basin are either snow or rain-dominated. Figure 9 shows a map of snow-dominated grid cells in the Sacramento–San Joaquin basin under 1961–1990 conditions (ΔT = 0°C) and selected incremental temperature increases. This shows that the highest-elevation regions in the southern Sierra Nevada remain snow-dominated even under a 5°C warming, though most of the snow-dominated area vanishes in the northern portion

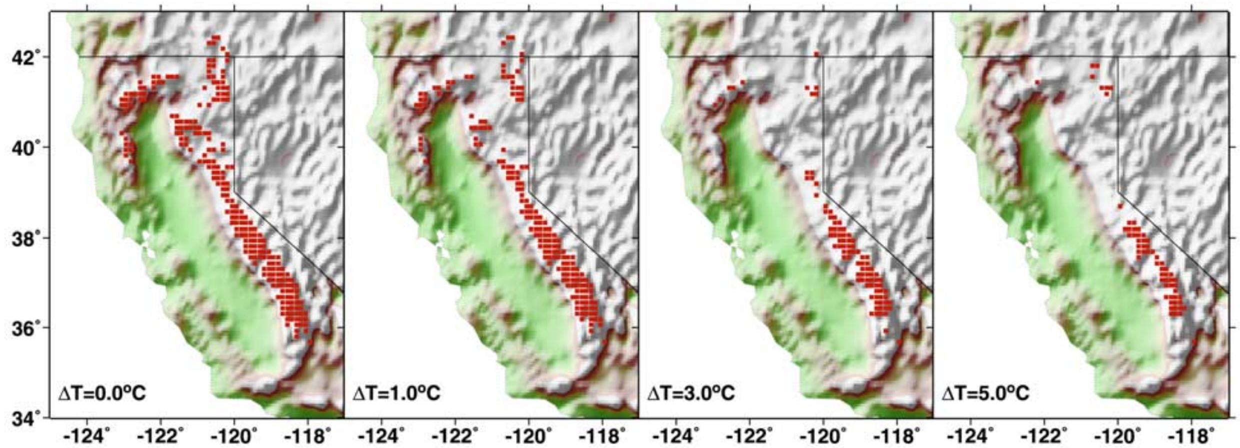

Figure 9. Snow-dominated grid cells, shown in red, under different incremental temperature increases above 1961–1990 levels, for the study basin shown in Figure 1.

(roughly north of Lake Tahoe at the vertex of the eastern state border) with a temperature increase of 3°C over 1961–1990 levels. Referring to Figure 7 it is evident that once a 3°C temperature increase has occurred, nearly two thirds of the water stored as snow on 1 April is lost, highlighting that additional timing changes, while potentially large, will affect smaller volumes of water.

[37] Figure 10 recasts the data from Figure 9 as the snow-dominated area for the 400 m elevation zones for each temperature increase for the north and south regions. As temperatures increase by 1°C above 1961–1990 levels, elevations between 1600 and 2000 m, historically about 60% snow-dominated in the north, will drop to 30% snow-dominated. In the south, elevations between 2000 and 2400 m, historically 100% snow-dominated, will lose about 10% of their snow-dominated area with a 1°C increase. As temperatures rise from 1° to 2°C above 1961–1990 levels, very little area below 2000 m is snow-dominated either in the north or south, and the 2000–2400 m zone drops to about 60% of its snow-dominated area in the south. With a 3°C increase most of the 2000–2400 m zone ceases to be snow-dominated in the north, and about half of the snow-dominated area in the south is lost. As shown in Figure 7, there is very little area in the northern Sierra above 2400 m, though the small amount that is remains snow-dominated. In the south, zones with elevations above 2800 m are

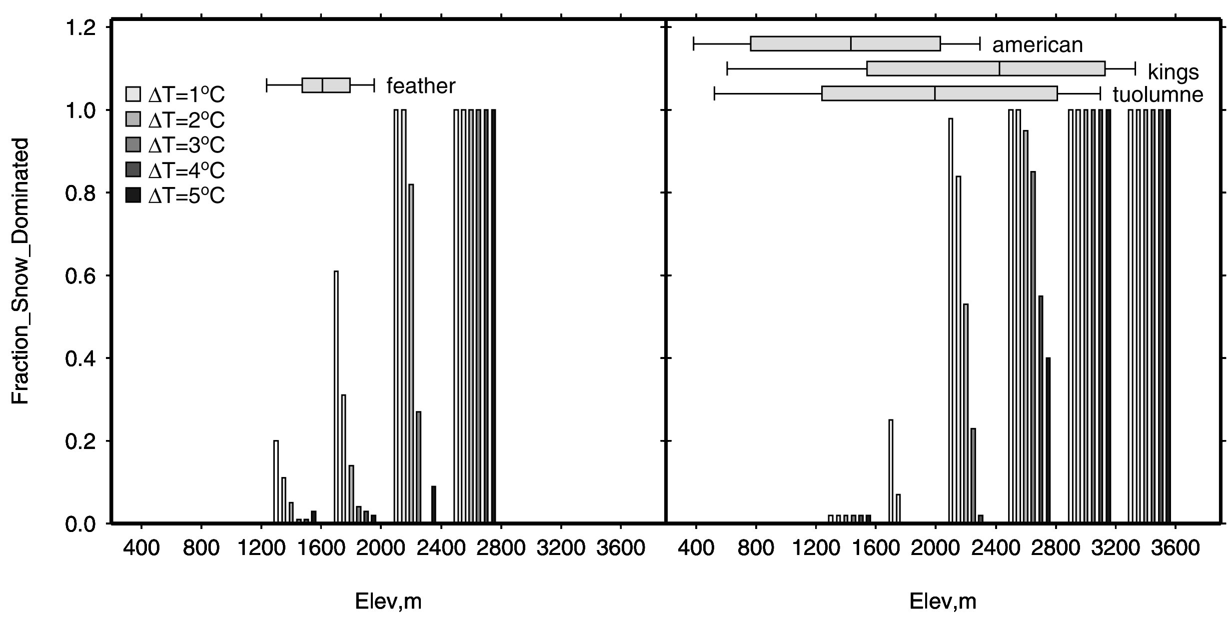

Figure 10. Fraction of snow dominated area within 400 m elevation zones for the (left) north and (right) south. The open (leftmost) bar in each elevation zone indicates the 1961–1990 level. Hypsometric data for the four key basins are as in Figure 5.

generally unaffected even by a 5°C temperature increase, though these represent only a small area, and a small volume of water stored as snow (Figure 7).

4. Conclusions

[38] The warming experienced in recent decades has caused measurable shifts toward earlier streamflow timing in California. Under future warming, further shifts in streamflow timing are projected for the rivers draining the western Sierra Nevada, including the four considered in this study. These shifts and their projected increases through the end of the 21st century will have dramatic impacts on California's managed water system.

[39] We show that for the 1950–1999 period, historical CT trends (as simulated by the VIC model) at four key stream locations, representing outflows for large drainage basins that are topographically complex, are currently too small to be statistically significantly different from natural climate variability. In other words, the 1950–1999 CT shifts are not yet statistically attributable to external (such as greenhouse gas driven) influences on climate. This is established by comparing estimated actual trends to maximum trends likely to arise from natural climate variability, as estimated from a surface hydrology model driven by meteorology from a multicentury GCM control simulation. This comparison of observed trends to trends expected from natural variability is distinct from tests of statistical significance, which compare observed trends to interannual variability within observed data. While attribution of externally forced climate change was found to be negative on 50-year timescale (1950–1999), it could potentially be positive when considering CT shifts over a longer historic period, because the amplitude of noise on longer timescales declines rapidly. In addition, while attribution was not positive for 1950–1999 for these four large basins, this does not indicate that CT trends for smaller, snow-dominated subareas would not be potentially attributable to external forcing.

[40] Future CT trends were projected for these four key sites in an earlier study. We estimate that these projected trends toward earlier CT will be confidently attributable to external forcing within the next 1 to 4 decades (by early to mid-21st century) if we follow a higher greenhouse gas emissions pathway (SRES A2), or 4 to 8 decades (by mid- to late-21st century) under a lower emissions future (SRES B1). We also find that the projected CT shift for the more vulnerable midelevations (2000–2400 m) may need to exhibit greater trends to achieve statistical confidence than higher elevations.

[41] We evaluate the sensitivity of different elevation zones in the western Sierra Nevada (Sacramento–San Joaquin basin). The greatest CT shifts will occur in areas with climatological winter temperatures from −2°C to −4°C. When considering elevation as a defining characteristic, at elevations of 1600–2400 m even low levels of temperature increases (1°–2°C) exhibit CT shifts of 10–15 days earlier in the year. Since a temperature rise of this magnitude is anticipated by even the most conservative future projections, adaptation for the resulting shifts in streamflow timing should be pursued. Under levels of warming above 3°C (projected under mid-to-high greenhouse gas emissions scenarios), CT shifts exceed 30 days for elevations of 2000–2800 m, and almost all zones below 2000 m become rain-dominated, essentially eliminating snow influence on streamflow timing for all northern Sierra Nevada streams. At elevations in the range of 2000–2800 m, the greatest streamflow timing impact is projected under the greatest warming considered here (5°C), with average shifts in timing exceeding 40 days earlier in the north and 45 days in the south.

[42] We show that, for areas south of latitude 39.5°N, the greatest changes in streamflow timing will occur at elevations that currently store the greatest amount of snow at the end of the winter. The loss of this immense amount of stored water, and its earlier arrival at the downstream reservoirs, will pose a serious challenge to water managers as they try to meet competing objectives of flood control and water supply.

[43] **Acknowledgments.** Mike Wehner of Lawrence Berkeley Laboratory assisted with the assembling and quality control of the PCM simulation output. The National Center for Atmospheric Research is acknowledged for providing their data for analysis, the Program for Climate Model Diagnosis and Intercomparison (PCMDI) for collecting and archiving the model data, the JSC/CLIVAR Working Group on Coupled Modeling (WGCM) and their Coupled Model Intercomparison Project (CMIP) and Climate Simulation Panel for organizing the model data analysis activity, and the IPCC WG1 TSU for technical support. The IPCC Data Archive at Lawrence Livermore National Laboratory is supported by the Office of Science, U.S. Department of Energy. This work was supported in part by MGC 04-04 under a grant from the Regents of the University of California/California Energy Commission, Public Interest Energy Research program.

References

Abdulla, F. A., D. P. Lettenmaier, E. F. Wood, and J. A. Smith (1996), Application of a macroscale hydrologic model to estimate the water balance of the Arkansas–Red River Basin, *J. Geophys. Res.*, *101*, 7449–7459.

Bales, R. C., N. P. Molotch, T. H. Painter, M. D. Dettinger, R. Rice, and J. Dozier (2006), Mountain hydrology of the western United States, *Water Resour. Res.*, *42*, W08432, doi:10.1029/2005WR004387.

Brekke, L. D., N. L. Miller, K. E. Bashford, N. W. T. Quinn, and J. A. Dracup (2004), Climate change impacts uncertainty for water resources in the San Joaquin River Basin, California, *J. Am. Water Resour. Assoc.*, *40*, 149–164.

Cayan, D. R., S. A. Kammerdiener, M. D. Dettinger, J. M. Caprio, and D. H. Peterson (2001), Changes in the onset of spring in the western United States, *Bull. Am. Meteorol. Soc.*, *82*, 399–415.

Cayan, D. R., E. P. Maurer, M. D. Dettinger, M. Tyree, and K. Hayhoe (2007), Climate change scenarios for the California region, *Clim. Change*, in press.

Christensen, N. S., A. W. Wood, N. Voisin, D. P. Lettenmaier, and R. N. Palmer (2004), The effects of climate change on the hydrology and water resources of the Colorado River Basin, *Clim. Change*, *62*, 337–363.

Covey, C., K. M. AchutaRao, U. Cubasch, P. Jones, S. J. Lambert, M. E. Mann, T. J. Phillips, and K. E. Taylor (2003), An overview of results from the Coupled Model Intercomparison Project, *Global Planet. Change*, *37*, 103–133.

Dettinger, M., K. Redmond, and D. Cayan (2004), Winter orographic precipitation ratios in the Sierra Nevada: Large-scale atmospheric circulations and hydrologic consequences, *J. Hydrometeorol.*, *5*, 1102–1116.

Gleick, P. H. (1987), Regional hydrologic consequences of increases in atmospheric CO_2 and other trace gases, *Clim. Change*, *10*, 137–160.

Hamlet, A. F., P. W. Mote, M. P. Clark, and D. P. Lettenmaier (2005), Effects of temperature and precipitation variability on snowpack trends in the western U.S., *J. Clim.*, *18*, 4545–4561.

Hayhoe, K., et al. (2004), Emissions pathways, climate change, and impacts on California, *Proc. Natl. Acad. Sci.*, *101*, 12,422–12,427.

Hodgkins, G. A., R. W. Dudley, and T. G. Huntington (2003), Changes in the timing of high flows in New England over the 20th century, *J. Hydrol.*, *278*, 244–252.

Howat, I. M., and S. Tulaczyk (2005), Climate sensitivity of spring snowpack in the Sierra Nevada, *J. Geophys. Res.*, *110*, F04021, doi:10.1029/2005JF000356.

Knowles, N., and D. R. Cayan (2004), Elevational dependence of projected hydrologic changes in the San Francisco estuary and watershed, *Clim. Change*, *62*, 319–336.

Knowles, N., M. Dettinger, and D. Cayan (2006), Trends in snowfall versus rainfall for the western United States, *J. Clim.*, *19*, 4545–4559.

Lettenmaier, D. P., and T. Y. Gan (1990), Hydrologic sensitivities of the Sacramento–San Joaquin River Basin, California, to global warming, *Water Resour. Res.*, *26*, 69–86.

Liang, X., D. P. Lettenmaier, E. Wood, and S. J. Burges (1994), A simple hydrologically based model of land surface water and energy fluxes for general circulation models, *J. Geophys. Res.*, *99*, 14,415–14,428.

Liang, X., D. P. Lettenmaier, and E. F. Wood (1996), One-dimensional statistical dynamic representation of subgrid spatial variability of precipitation in the two-layer variable infiltration capacity model, *J. Geophys. Res.*, *101*, 21,403–21,422.

López-Moreno, J. I., and J. M. García-Ruiz (2004), Influence of snow accumulation and snowmelt on streamflow in the central Spanish Pyrenees, *Hydrol. Sci.*, *49*, 787–802.

Lundquist, J. D., and A. L. Flint (2006), Onset of snowmelt and streamflow in 2004 in the western United States: How shading may affect spring streamflow timing in a warmer world, *J. Hydrometeorol.*, *7*, 1199–1217.

Lundquist, J. D., D. R. Cayan, and M. D. Dettinger (2004), Spring onset in the Sierra Nevada: When is snowmelt independent of elevation?, *J. Hydrometeorol.*, *5*, 327–342.

Maurer, E. P. (2007), Uncertainty in hydrologic impacts of climate change in the Sierra Nevada, California under two emissions scenarios, *Clim. Change*, *82*, 309–325, doi:10.1007/s10584–10006–19180–10589.

Maurer, E. P., and P. B. Duffy (2005), Uncertainty in projections of streamflow changes due to climate change in California, *Geophys. Res. Lett.*, *32*, L03704, doi:10.1029/2004GL021462.

Maurer, E. P., G. M. O'Donnell, D. P. Lettenmaier, and J. O. Roads (2001), Evaluation of the land surface water budget in NCEP/NCAR and NCEP/DOE reanalyses using an off-line hydrologic model, *J. Geophys. Res.*, *106*, 17,841–17,862.

Maurer, E. P., A. W. Wood, J. C. Adam, D. P. Lettenmaier, and B. Nijssen (2002), A long-term hydrologically-based data set of land surface fluxes and states for the conterminous United States, *J. Clim.*, *15*, 3237–3251.

Mote, P. W., A. F. Hamlet, M. P. Clark, and D. P. Lettenmaier (2005), Declining mountain snowpack in western North America, *Bull. Am. Meteorol. Soc.*, *86*, 39–49.

Nijssen, B., D. P. Lettenmaier, X. Liang, S. W. Wetzel, and E. Wood (1997), Streamflow simulation for continental-scale basins, *Water Resour. Res.*, *33*, 711–724.

Nijssen, B., G. M. O'Donnell, A. F. Hamlet, and D. P. Lettenmaier (2001), Hydrologic sensitivity of global rivers to climate change, *Clim. Change*, *50*, 143–175.

Payne, J. T., A. W. Wood, A. F. Hamlet, R. N. Palmer, and D. P. Lettenmaier (2004), Mitigating the effects of climate change on the water resources of the Columbia River Basin, *Clim. Change*, *62*, 233–256.

Peck, E. L. (1976), Catchment modeling and initial parameter estimation for the National Weather Service River Forecast System, *NOAA Tech. Memo. NWS HYDRO-31*, Silver Spring, Md.

Regonda, S. K., B. Rajagopalan, M. Clark, and J. Pitlick (2005), Seasonal cycle shifts in hydroclimatology over the western United States, *J. Clim.*, *18*, 372–384.

Santer, B. D., et al. (2006), Forced and unforced ocean temperature changes in Atlantic and Pacific tropical cyclogenesis regions, *Proc. Natl. Acad. Sci.*, *103*, 13,905–13,910.

Smith, M. B., D. Laurine, V. Koren, S. Reed, and Z. Zhang (2003), Hydrologic model calibration in the National Weather Service, in *Calibration of Watershed Models*, *Water Sci. Appl. Ser.*, vol. 6, edited by Q. Duan et al., pp. 133–152, AGU, Washington, D. C.

Stewart, I. T., D. R. Cayan, and M. D. Dettinger (2004), Changes in snowmelt runoff timing in western North America under a "business as usual" climate change scenario, *Clim. Change*, *62*, 217–232.

Stewart, I. T., D. R. Cayan, and M. D. Dettinger (2005), Changes toward earlier streamflow timing across western North America, *J. Clim.*, *18*, 1136–1155.

Tanaka, S. K., T. Zhu, J. R. Lund, R. E. Howitt, M. W. Jenkins, M. A. Pulido, M. Tauber, R. S. Ritzema, and I. C. Ferreira (2006), Climate warming and water management adaptation for California, *Clim. Change*, *76*, 361–387.

Van Rheenen, N. T., A. W. Wood, R. N. Palmer, and D. P. Lettenmaier (2004), Potential implications of PCM climate change scenarios for Sacramento–San Joaquin River Basin hydrology and water resources, *Clim. Change*, *62*, 257–281.

Vicuna, S., E. P. Maurer, B. Joyce, J. A. Dracup, and D. Purkey (2007), The sensitivity of California water resources to climate change scenarios, *J. Am. Water Resour. Assoc.*, *43*, 482–498, doi:10.1111/j.1752-1688.2007.00038.

Washington, W. M., et al. (2000), Parallel Climate Model (PCM) control and transient simulations, *Clim. Dyn.*, *16*, 755–774.

Wood, A. W., E. P. Maurer, A. Kumar, and D. P. Lettenmaier (2002), Long-range experimental hydrologic forecasting for the eastern United States, *J. Geophys. Res.*, *107*(D20), 4429, doi:10.1029/2001JD000659.

Wood, A. W., L. R. Leung, V. Sridhar, and D. P. Lettenmaier (2004), Hydrologic implications of dynamical and statistical approaches to downscaling climate model outputs, *Clim. Change*, *62*, 189–216.

Zhu, C., D. W. Pierce, T. P. Barnett, A. W. Wood, and D. P. Lettenmaier (2004), Evaluation of hydrologically relevant PCM climate variables and large-scale variability over the continental U.S., *Clim. Change*, *62*, 45–74.

C. Bonfils, School of Natural Sciences, University of California, Merced, CA 95344, USA. (bonfils2@mail.llnl.gov)

D. Cayan, Water Resources Division, U.S. Geological Survey, 201 Nierenberg Hall, La Jolla, CA 92093-0224, USA. (dcayan@ucsd.edu)

P. B. Duffy, Lawrence Livermore National Laboratory, Livermore, CA 94551-0808, USA. (pduffy@llnl.gov)

E. P. Maurer, Civil Engineering Department, Santa Clara University, Santa Clara, CA 95053-0563, USA. (emaurer@engr.scu.edu)

I. T. Stewart, Environmental Studies Program, Santa Clara University, Santa Clara, CA 95053, USA. (istewartfrey@scu.edu)